



Akademie věd České republiky

Teze doktorské disertační práce
k získání vědeckého titulu "doktor věd"
ve skupině věd fyzikálně-matematických

**Magnetic properties of high temperature
superconductors**

název disertace

Komise pro obhajoby doktorských disertací v oboru
Fyzika kondenzovaných systémů

Jméno uchazeče **RNDr. Miloš Jirsa, CSc.**

Pracoviště uchazeče **Fyzikální ústav AVČR Praha**

Místo a datum **Praha, 1. 7. 2004**

Preface

This thesis consists of 24 publications dealing with various aspects of vortex physics in high- T_c superconductors. The articles were divided into 4 groups devoted to (i) Effect of dynamic relaxation (6 articles); (ii) $J(B)$ performance of untwinned bulk RE-123 superconductors (8 articles); (iii) Twin structure effects in bulk RE-123 compounds (4 papers); and (iv) Granular superconductors (6 papers).

The study of high- T_c superconductors started in our group in 1987, soon after the discovery of superconductivity in $\text{YBa}_2\text{Cu}_3\text{O}_{7-\delta}$. It was the first high- T_c material fabricated by our chemists, firstly in the form of ceramics, soon after that also in the form of single crystals.

The papers collected in the thesis cover the period since 1990 till now. Most of them were published in the Institute of Physics ASCR, based on the experimental data detected and analyzed on our own facilities in IP ASCR. As regards samples, YBaCuO single crystals were produced in our Institute, some were provided by M. Koblischka from Institute of Physics in Stuttgart, some by T. Nishizaki from Institute for Material Research of Tohoku University, Sendai, Japan; a number of twin-free $\text{DyBa}_2\text{Cu}_3\text{O}_y$ single crystals were offered by M. Koblischka. Some $\text{DyBa}_2\text{Cu}_3\text{O}_y$ single crystals were irradiated in Laboratory CRISMAT, University of Caen, France, and in Nuclear Laboratory in Berlin, Germany, in cooperation with the Institute of Physics in Stuttgart, Germany. Mg- and Cd- doped $\text{YBa}_2\text{Cu}_3\text{O}_y$ ceramics were produced in Aristotle University in Thessaloniki, Greece. We had monocore BiSrCaCuO tapes from University of Geneva, Switzerland, the Institute of Electrical Engineering of SAS, Bratislava, Slovakia, and NKT Brøndby, Denmark. $\text{YBa}_2\text{Cu}_3\text{O}_y$ thin films were produced during the working stay of the author in the Institute of Thin Films and Interfaces in Jülich, Germany; the first ‘model’ thin film structure was produced at Chalmers University Stockholm, Sweden, the newest series of samples of this kind were fabricated by doctoral student V. Yurchenko during his working stays in the Institute of Thin Films and Interfaces in Jülich, Germany. Richness of bulk melt-textured materials and especially experimental data of them were available from Superconductivity Research Laboratory of the International Superconductivity Technology Center (SRL/ISTEC) in Tokyo and its branch in Morioka.

Our main experimental facility has been steadily a vibrating sample magnetometer (VSM) PAR 155, recently upgraded to LakeShore 4500, installed in helium cryostat (2 – 300 K) and equipped with a conventional laboratory electromagnet (± 2 Tesla). In the beginning of the research (1987), the author designed and constructed a special sweeping unit for the VSM that later enabled extensive field-sweep experiments and recently also series of minor loop measurements on tapes, ‘model’ thin films and other magnetic samples. Alternatively, a

commercial SQUID magnetometer MPMS5 (± 5 Tesla) in Department of magnetic oxides and superconductors has been used. During 3 months study stay at Free University of Amsterdam, Netherlands, in 1993, the author used torsion magnetometer for angular measurements of high- T_c single crystals. Some experiments were performed by means of the VSM of Oxford Instruments (± 5 Tesla) in Imperial College, Centre for High Temperature Superconductivity, London, GB, and another Oxford Instruments set-up (± 14 Tesla) in Institute for Material Research of Tohoku University, Sendai, Japan. A number of SQUID measurements was performed during the authors visits in SRL/ISTEC, Tokyo. Further huge quantity of SQUID data got available through the authors collaboration with M. Muralidhar from the same institution. Magneto-optical measurements were performed at University of Oslo, Norway. Data for some articles were collected and reconstructed from literature, in order to make the conclusions as general as possible.

The above survey of experimental technique indicates that our work in the field of high- T_c superconductivity has been mainly focused on magnetic properties of various types of high temperature superconductors. Here it should be pointed out that magnetic moment in superconductors is usually, and in our studies exclusively, a magnetic moment induced by a change of external magnetic field. This fact is reflected in a high sensitivity of the measured data on magnetic history of the investigated sample and, consequently, also the measuring method. We were rather lucky when starting our experiments just with VSM that offered the best control over measurement conditions of all magnetic measurement methods. Only torsion magnetometer came close. Both the latter methods enabled continuous measurements in the field sweeping mode, which has proved to be crucial for the study of high- T_c compounds.

In the first part, the effect of field sweep on irreversible magnetization is described, as extensively studied on single crystals of Y-123 and Dy-123. This research resulted in development of a new experimental method called dynamic relaxation. The second part is devoted to the phenomenological description of the characteristic feature (called sometimes fishtail) of magnetic hysteresis loops of untwinned bulk RE-123 superconductors and to the search for novel effective vortex pinning defects enhancing the fishtail effect. The third part deals with twin structure activity and its effect on magnetic hysteresis loop. Finally, our research of the induced magnetic moment in granular superconductors is reported in section four.

1. The effect of dynamic relaxation

Soon after the discovery of high- T_c superconductivity, we started with investigation of their magnetic properties. Extensive measurements of $YBa_2Cu_3O_y$ single crystals led to our discovery that magnetic hysteresis loop is sensitive to the field sweep rate. The correlation

between hysteresis loop size and magnetic field sweep rate^{1-1,1-2} was analyzed and analytically described. Later on, this relationship was quantitatively expressed in the effective relaxation time associated with the hysteresis loop size (magnetic moment value) measured at the given field sweep rate^{1-3,1-4}.

In classical relaxation experiments at a constant magnetic field, the data are detected starting from a rather high time (typically hundreds seconds after the field stop. Interpretation of such data suffers from the relaxation time scale origin determination uncertainty. This problem was solved by expressing the measured classical relaxation $M(t)$ dependence in terms of the associated M vs dM/dt or dB/dt dependence. In this case, both quantities could be exactly determined from the experimental $M(t)$ curve and the need of time origin was eliminated. Moreover, as dM/dt is related to dB/dt through a constant factor χ_0/μ_0 , where χ_0 is the differential susceptibility and μ_0 is permeability of vacuum, the classical relaxation experiment, expressed in terms of M vs dM/dt , could be directly combined with measurements of hysteresis loops expressed in terms of M vs. dB/dt (see Figs. 1 and 2). The only unknown in the problem was the differential susceptibility, χ_0 , that is related to sample dimensions.^{1-3,1-4} In this way, the measurement of full hysteresis loops with different field sweep rates, introduced into practice^{1-4,1-5,1-6} as **dynamic relaxation**, became a fast alternative to classical relaxation experiments. By measuring two full hysteresis loops at slightly different field sweep rates, relaxation data in the whole field range can be obtained at once at a rather short time. Moreover, the time scale of dynamic relaxation was complementary to the range of classical relaxation times, lying below these times, in the sub-second range.

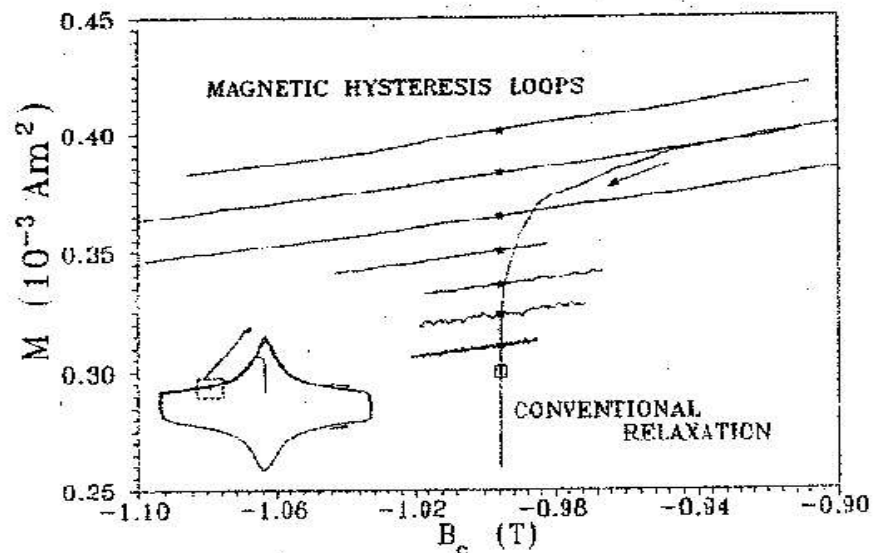


Fig. 1. A series of MHLs measured at different field sweep rates, combined with a conventional relaxation started from the second run from top.

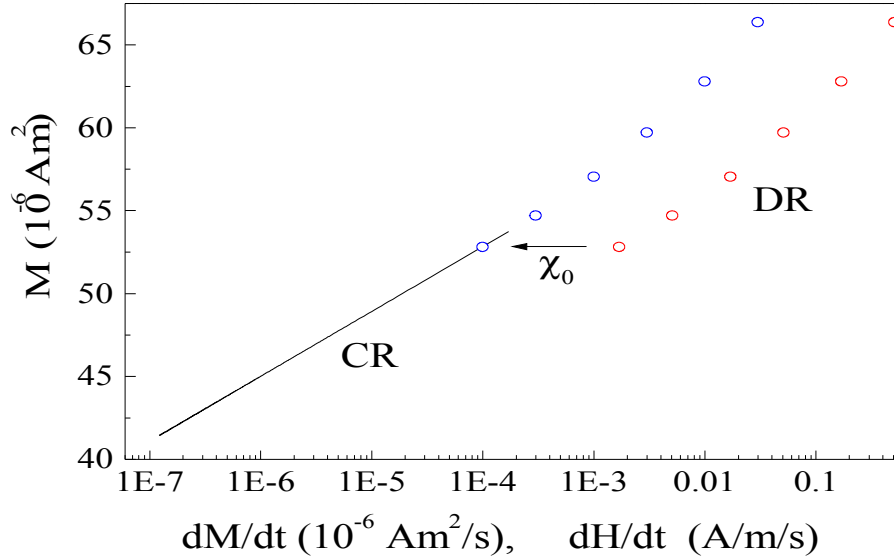


Fig. 2. Combined classical and dynamic relaxation data in terms of M vs. dM/dt , resp. M vs. dH/dt

Because magnetic moment M is according to Bean's critical state model related to the super-current density, J_c , through a geometrical factor^{1-4,1-5,1-6} and $dB/dt \propto E$, the electric field in the superconductor, both types of relaxation experiments can be related also to transport current experiments (I - V curves). Until that time, it was not clear why the transport data gave so different J_c values from those from magnetic measurements. Only after taking into account their respective relaxation states (relaxation time windows), the J_c values obtained from different experiments were brought into accord.

The dynamic relaxation has been extensively used for collecting experimental data for various material characterisation schemes, like General Inversion Scheme¹, or E-J-B surface².

2. $J(B)$ performance of untwinned bulk RE-123 super-conductors

Typical feature of most bulk RE-Ba₂Cu₃O_y (RE=rare earth, RE-123) materials is a peak on magnetic hysteresis loops (MHL) at intermediate magnetic fields. This characteristic enhancement of magnetic moment or the associated super-current density is called fishtail (according to the specific shape of the MHL) or second peak effect (second to the central peak at zero magnetic field). In clean Y-123 single crystals this phenomenon was identified with oxygen deficient state and attributed to vortex pinning on point-like disorder of oxygen depleted clusters of the superconducting matter.³⁻⁵ Later on, it was found that a similar effect can be induced also by other types of structural fluctuations, e.g. by nanoscopic LRE/Ba solid solution clusters.

Despite of the numerous attempts to explain the phenomenon in terms of classical principles, up to now no satisfactory agreement on its origin has been found. We succeeded in finding a very good phenomenological description of the phenomenon. It is based on the

model of a general thermally activated flux creep introduced by Perkins *et al.*^{6,7} They expressed activation energy as a product of a current-dependent term and a field- and temperature- dependent “background”, $U(T,B,J)=U_0(T,B)F(J/J_0)$. From the experimentally observed scaling property the authors deduced that both characteristic parameters U_0 and J_0 were power functions of B . The extensive (dynamic) relaxation experiments on Tm-123 single crystals showed that the function $F(J)$ was logarithmic, $J_0 \propto B$, and $U_0 \propto 1/B$. Our own measurements on various RE-123 single crystals and our analysis of extensive data published in literature led us to the conclusion that all available experimental data could be interpreted in terms of the above model with $U_0(B)$ dependence generalized as $U_0(B) \propto 1/B^n$ with n varying in the range 0.5 to 3.^{II-1,II-2,II-3} The model led to the phenomenological function^{II-1}

$$j(b)=b \exp[(1-b^n)/n] \quad , \quad (1)$$

where $j=J_c/J_{\max}=M/M_{\max}$, $b=B/B_{\max}$, and (B_{\max},J_{\max}) were coordinates of the second peak.

Evidently, function (1) goes to zero for $B \rightarrow 0$ (see Fig. 3). While the latter fact is close to reality in single crystals, especially at high temperatures (Fig. 3), it is not the case at low temperatures and in melt-textured samples at any temperature. In the latter cases a pronounced central peak appears that cannot be explained in terms of the Perkins’ model (Figs. 3 and 4).

After subtracting function (1) from the normalized experimental curves for various temperatures, we found that the central peak contribution to the MHL can be expressed by an

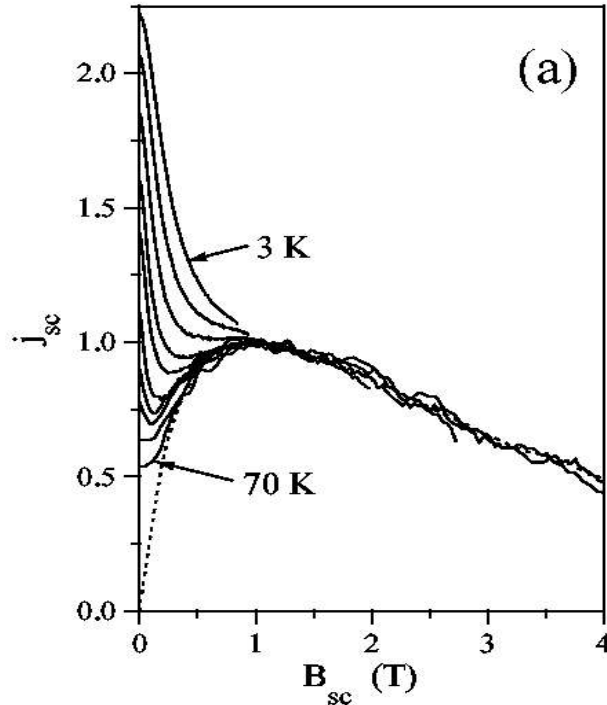


Fig. 3. The experimental $J_c/J_{\max}(B/B_{\max})$ dependence of a Dy-123 single crystal and its fit by means of Eq. (1).

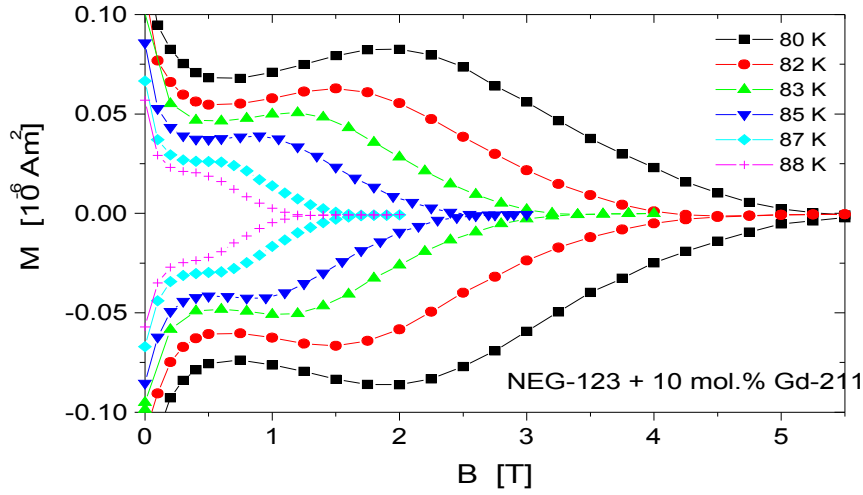


Fig. 4. Magnetic hysteresis loop of a melt-textured (NdEuGd)-123+10mol% Gd-211.

exponentially decay- ing function of field^{II-1,II-4,II-5},

$$J(B)=J_1 \exp(B/B_L) \quad , \quad (2)$$

where J_1 is the height of the central peak and B_L the field scale. Combination of Eqs. (1) and (2),

$$J(B)=J_1 \exp(B/B_L)+J_{max}B/B_{max}\exp[(1-(B/B_{max})^n)/n], \quad (3)$$

is able to fit MHLs (or associated $J(B)$ dependencies) in practically all bulk RE-123 twin-free samples, in all temperatures and fields, with a surprisingly high precision (Fig. 5).

The fitting parameters are usually B_L , B_{max} , J_{max} , and n , while J_1 is taken from experiment. In the case that the second peak is well separated from the central one, B_{max} and J_{max} can be directly determined from the experiment and only B_L and n are left free. Even in this case the fit is excellent^{II-4} (Fig. 5). In most cases $B_L \ll B_{max}$ so that the first term decays fast and is usually nearly zero at B_{max} .

Recent experiments on melt-textured samples with various sizes of secondary phase particles (just sent for publication in SUST 2004) showed that B_L scales with temperature in a similar manner as B_{max} (and irreversibility field, B_{irr}). Thus, the effect of the low-field pinning mechanism stays limited to the field range below the second peak in a broad range of temperatures. Only at very high temperatures the small point-like defects lose their efficiency in account of much larger secondary phase particles, the second peak vanishes and the whole MHL is due to only the first term in Eq. (3).

The exponential decay of super-currents at low fields due to vortex pinning on large particles was also supported by our theoretical model of pinning on large normal defects.^{II-5}

The splitting of the $J(B)$ dependence into two additive terms enabled us to study in detail relaxation properties of both respective pinning mechanisms^{II-6,II-7}. We measured total MHLs with different field sweep rates, by fitting these curves with model

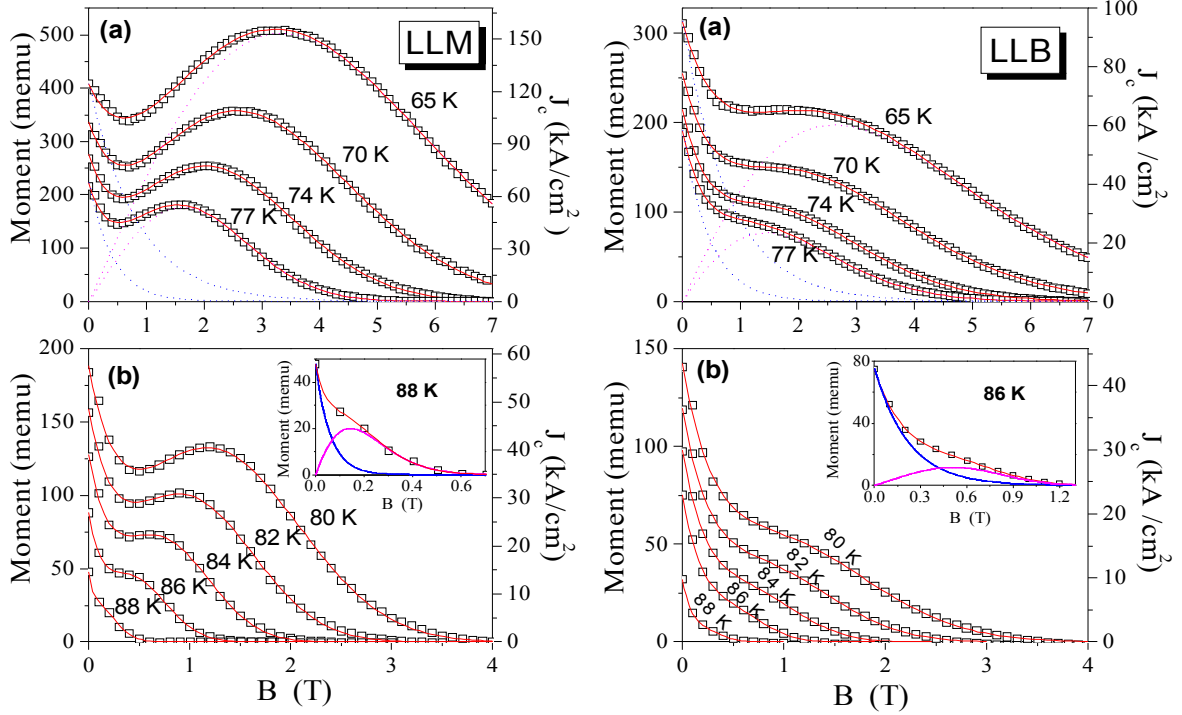


Fig. 5. Fit by means of Eq. (3) (red solid curves) of two types of experimental $M(B)$ dependences (symbols) of two melt-textured (Nd,Eu,Gd)-123 samples, LLM and LLB. The dotted lines in the upper panels indicate the individual terms from Eq. (3).

function (3), we separated the central and second peaks for different field sweep rates, then analyzed the relaxation behavior of the individual contributions, calculated the corresponding normalized dynamic relaxation rates,

$$Q_i(B) = \Delta \ln M_j / \Delta \ln (dB/dt)_j, \quad (4)$$

where the subscript $i=1,2$ corresponded to the central and second peak, respectively, and subscripts $j=1,2$ corresponded to different field sweep rates. Finally, these relaxation rates could be combined into the total one as^{II-6}

$$Q(B) = [Q_1(B)J_1 + Q_2(B)J_2] / (J_1 + J_2), \quad (5)$$

where J_1 and J_2 represent the first and second term in Eq. (3), respectively. Analysis of Eq. (1) showed that $n = d \ln M / d \ln B$ at the high-field inflexion point of the second peak (Fig. 6).^{II-7}

It is commonly observed that MHLs of RE-123 bulk superconductors scale with temperature. It means that all the normalized curves for different temperatures fall onto one universal curve. As a result, the position of the inflexion point does not change and n stays constant. Vice versa, constant n is a sign of well scaling MHLs. In Fig. 6 one can see that in such a case the inflexion point lies on the line running from the coordinate origin with slope $1/e$. From the Perkins' model it follows that

$$Q = \gamma_E (1 - d \ln M / d \ln B), \quad (6)$$

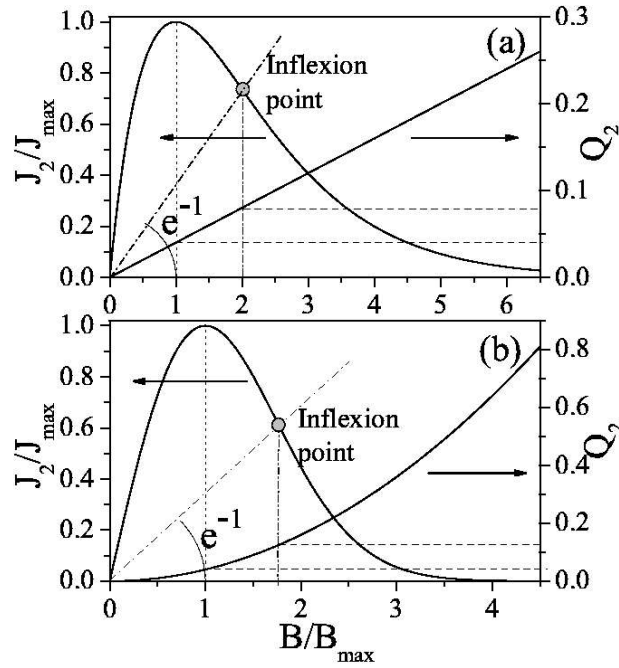


Fig. 6. Plots of theoretical $j(b)$ and $Q_2(b)$ curves (Eqs. (1) and (7)) for $n=1$ (a) and $n=2$ (b).

where γ_E is a temperature independent parameter. Combining Eqs. (1) and (6), we get^{II-6,II-7}

$$Q_2 = \gamma_E (B/B_{\max})^n \quad (7)$$

Similarly, for the central peak $Q_1 = \gamma_E (1 + B/B_L)$. Although both the individual relaxation rates are increasing functions of B , in the combination (5) they exhibit only a slightly fluctuating field dependence below B_{\max} .^{II-7} Note that $Q = \gamma_E$ at any extreme of $M(B)$. Therefore, going from the central peak maximum to the minimum between both peaks and finally to the second peak maximum, $Q(B)$ fluctuates around γ_E value (see Fig. 7). The minimum value of $Q(B)$ lies approximately in the middle between the dip and the second peak maximum of the $M(B)$ or

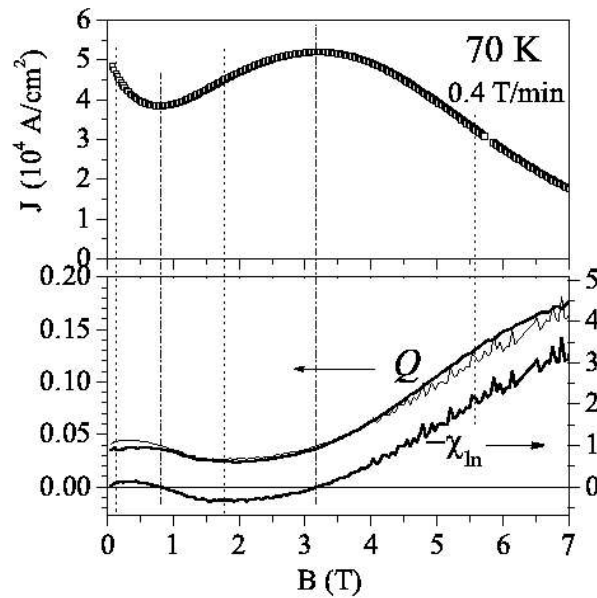


Fig. 7. Comparison of the MHL shape (upper panel) with the corresponding normalized dynamic relaxation rate, Q , (lower panel)

$J(B)$ dependence and its typical value, 0.02-0.03, relates to the typical γ_E lying between 0.03 and 0.05.

In the field dependence of pinning force density, $F=JB$, the effect of low-field pinning is suppressed as $F(B)$ goes to zero for $B \rightarrow 0$ (Fig. 8). $F(B)$ has only one extreme shifted to higher fields in comparison with the second peak on $J(B)$. Although $F(B)$ and $J(B)$ are simply functionally related and should be theoretically equivalent characteristics of the given material, in practice it is not the case. The experimental $F(B)$ curves scale much better with temperature (in a broader temperature range) than $J(B)$ ones (Fig. 9). This fact can be explained by a weaker effect of low-field pinning at fields around $F(B)$ maximum that lies significantly higher than that of $J(B)$.^{II-3,II-4}

As documented by Fig. 5, the analytical function (3) was very successful in fitting $J(B)$ performance of melt-textured samples. A broad variety of such samples have got available to us through collaboration of our group with Superconductivity Research Laboratory, ISTEK, Tokyo, where dr. M. Muralidhar specialized in developing top quality ternary melt-textured materials.

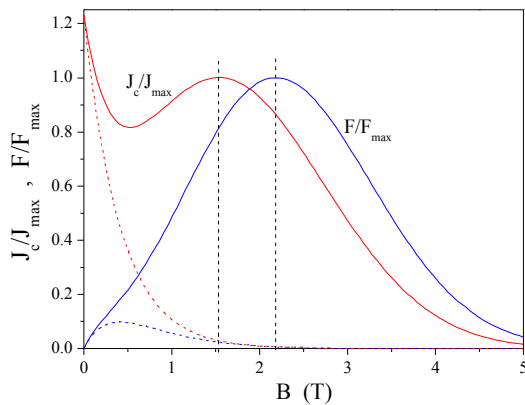


Fig. 8. Comparison of the peak position on $J(B)$ and $F(B)$ curves (calculated for experimental data of the melt-textured NEG-123 sample LLM at 77 K) and the respective range of operation of the ‘large’ particle pinning.

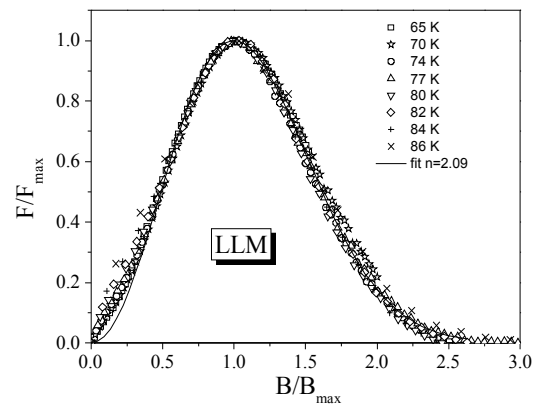


Fig. 9. Scaling of the experimental $F(B)$ data of the melt-textured NEG-123 sample LLM with respect to temperature.

Based on 5 subsequent study visits of the thesis author in Japan, over 45 common papers were published, either in well recognized international journals or in international conference proceedings (see the list of publications). In this research we participated by direct measurements, especially by means of VSM in IMR Sendai but also by measurements in Prague, by experimental data interpretation, discussions and revisions of the manuscripts.

One of the best achievements was recently reached in the attempt to further enhance the low-field vortex pinning by ‘large’ secondary phase particles.^{II-8} This type of pinning is

inversely proportional to a power of the mean particle size. Thus, the smaller the particles, the higher is the pinning effect. As usual, the matter is not so simple. The commercial secondary phase powders have an average size of about 3 μm , some secondary phases (e.g. Gd-211 or Eu-211) spontaneously form sub-micron particles during the melt-texturing process. In general, the way to nanoparticles is not easy, due to coarsening and alloying of the small particles into larger clusters. Therefore, the lowest particle size obtained by melt-texturing techniques has stood for a rather long time in the range of 0.1 μm . The newest significant step on this way was made by an attempt to further reduce the particle size by ball milling with Zr_2O_3 balls.¹¹⁻⁸ The commercial Gd-211 particles were milled for different times to get a series of powders with different particle sizes. The minimum size was about 70 nm, reached after 8 hours of milling. The effect on magnetic properties was, however inadequately dramatic. The structural analysis revealed not only particles above 70 nm but also much smaller ones, in the range 20-50 nm. All these particles contained a significant amount of Zr. Evidently, they developed from Gd-211 phase contaminated during the ball milling process. The inert Zr prevented the particle coarsening and represented something like a particle 'nucleus'. As a result, the super-current density at the remanent state dramatically increased at all high temperatures, up to a close vicinity of T_c ($\approx 94\text{-}96$ K). At 77 K, it increased more than twice (192 kA/cm²) in comparison to the previous record value (belonging to the same team and material group). At 90 K the trapped magnetic field after magnetization up to 5 T (proportional to the super-current density) was enough to perform levitation experiment with **liquid oxygen** (boiling point 90.2 K).¹¹⁻⁸ This result presents not only the perspective of designing contactless superconducting pumps for liquid oxygen and other liquid gasses for use in medicine and spacecraft technologies but it also provides the necessary safety reserve for operation with liquid nitrogen, at 77 K.

With minimization of the 'large' pinning defects one gets close to the limit of point-like pinning disorder. Therefore, behavior of such compounds is interesting also from the basic research point of view. We found that similar, even smaller, defects were also previously produced by fast neutron irradiation. In this case, avalanches of defects of a few nm in size were produced.^{8,9} Though in size very close to point-like defects, they enhanced super-currents preferentially at low fields, similarly to the nanometer-sized secondary phase particles. This raised the question of the actual mechanisms of vortex interaction with 'large' and point-like defects, and the origin of the second peak.

II.3. Twin structure effect in bulk RE-123 compounds

Most RE-Ba₂Cu₃O_y materials form twins in the (a-b) plane, systems of parallel zones with the material of interchanged *a* and *b* orientations. The boundaries between these zones are rather strong obstacles for flux front propagation. Therefore, magnetic flux penetrates

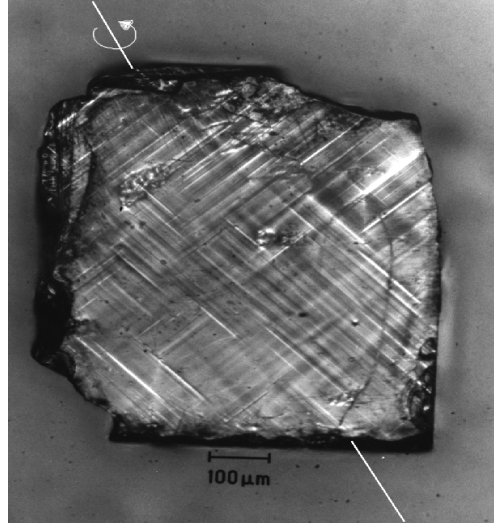


Fig. 10. Twin plane structure of a Nd-123 single crystal visualized in polarized light.

preferentially along twin planes. The typical twin configuration is shown in Fig. 10. Thus, the presence of a twin structure leads to another magnetic flux distribution than in samples without twins. Consequently, a different current distribution is observed.^{III-1} In practice, it is manifested by a modified magnetic hysteresis loop. In presence of a point-like disorder, the second peak is deformed. This effect appears only in the configuration with field parallel or close to the twin boundaries. With increasing angle between field and twin planes, the MHL becomes more and more regular and at some 20° the deformation due to twins completely disappears and the second peak follows Eq. (3). In other words, the Abrikosov vortices cross the twin planes like point-like defects^{III-1,III-2} (Fig. 11).

The exact mechanism of pinning is not yet clear but a combined action of twin boundaries and smaller defects in-between is evident. An extreme example is the melt-textured (Nd_{0.33}Eu_{0.38}Gd_{0.28})-123, where the channels between regular twin boundaries (about 80 nm apart) were filled by a substructure of lamellas parallel to the regular twins but of the width and period both about 3 nm (see Fig. 12). These lamellas were formed of nanoscopic clusters of slightly nonstoichiometric material.^{III-3} It happened in a narrow range of concentration ratios Nd:Eu:Gd around 33:38:28, where the super-conducting phase exhibited a structural frustration in the form of a fine, nanometer-scale zigzag structures or a lamellar

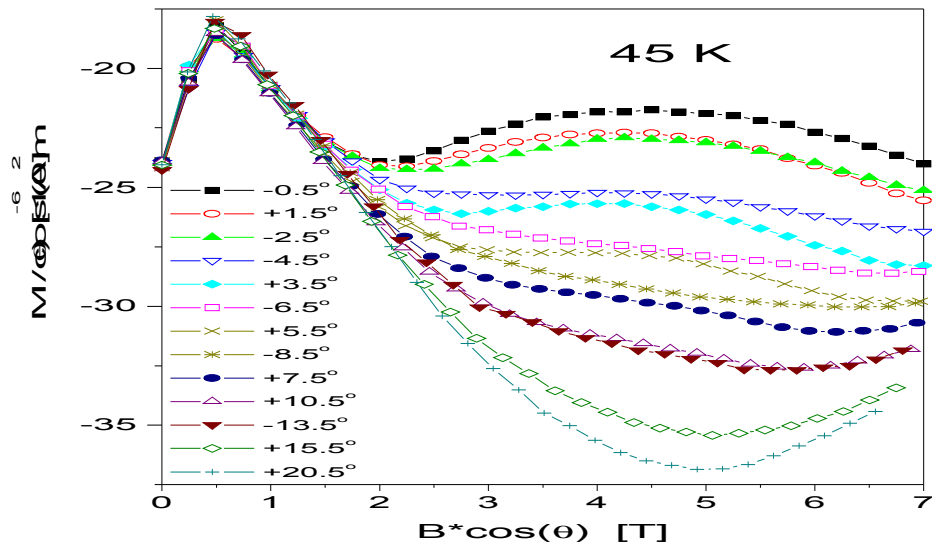


Fig. 11. Lower parts of MHLs measured on a Nd-123 single crystal at various angles between magnetic field and twin planes (c-axis) at 45 K. The plot shows c-axis components of magnetic moment and field.

substructure. As a result, the pinning efficiency at high fields was exceptionally enhanced, which led to a substantial increase of irreversibility field. At 77 K, B_{irr} reached 15 Tesla (Fig.13). It was about twice as much as in regular RE-123 compounds at the same temperature.^{III-3}

Even the regular twin planes themselves can be in some cases very helpful. At low temperatures their effect helps to ‘saturate’ the $J(B)$ dependence, which leads to a field-independent current density up to very high fields^{III-4} (Fig. 14).

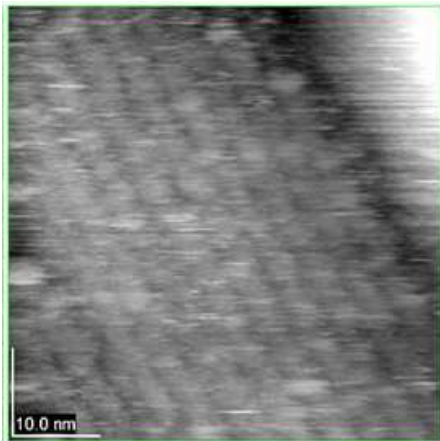


Fig. 12. STM image of the lamellar nanoscale pinning structure correlated with the regular twin plane structure (the dark line in the right upper corner).

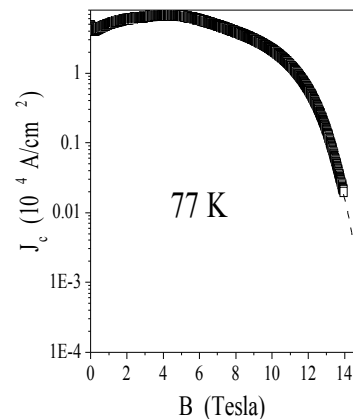


Fig. 13. $J(B)$ dependence of the sample showing the extrapolated irreversibility field of about 15 Tesla at 77 K.

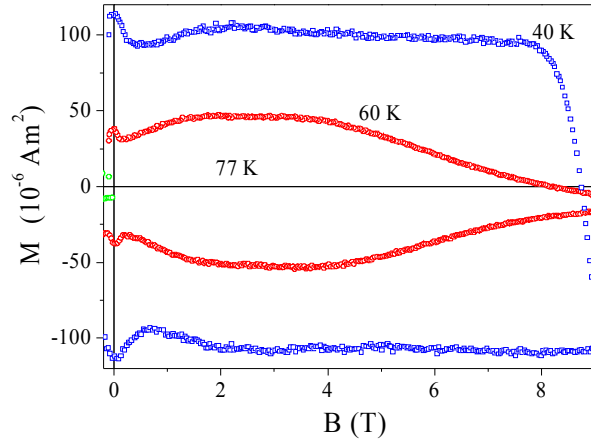


Fig. 14. Magnetic hysteresis loops of a twinned melt-textured Y-123 with regular twins, with field parallel to the twin planes (c-axis). The twin planes caused the MHL flattening, particularly evident at lower temperatures.

II.4. Granular superconductors

Polycrystalline or ceramical phase is the most common form of high-temperature superconductors. This section covers our activities in the research of bulk superconducting RE-123 ceramics, Bi-based tapes, and Y-123 thin film artificially granular structures.

Our joint research project with Aristotle University in Thessaloniki in years 1994-1997 aimed at investigation of the role of Mg and Cd doping of Y-123 ceramics. Properties of both series of the samples were similar. The samples doped by various amounts of Mg were reported in the paper [IV-1]. A non-monotonic dependence of the second peak position on the Mg concentration was observed, together with a similar but mirror effect on the penetration depth, λ_{ab} . The temperature dependence of λ_{ab} was at low temperatures linear. This was interpreted in terms of a spatial fluctuation of the superconducting phase in the rather heterogeneous system.¹⁰

$\text{Bi}_2\text{Sr}_2\text{Ca}_2\text{Cu}_3\text{O}_{10}/\text{Ag}$ (Bi-2223/Ag) tapes prepared in University of Geneve, Switzerland, were tested for anomalous induced currents characteristics.^{IV-2} Measuring magnetic hysteresis loops before and after the tape bending to a small diameter, contributions from inter- and intra-granular currents could be separated. In this way it was verified that the both observed anomalies (position of the central peak at positive decreasing fields and magnetic moment shift to positive values) were due to intergranular currents that after the tape bending (and destruction of the inter-grain links) disappeared, together with the associated anomalies. While the peak position was explained by demagnetization effects due to intragranular currents, the magnetic moment shift to positive values was attributed to a geometrical barrier at the grain edges.

Our measurements of the anomalous peak position in Bi-2223 tapes motivated Shantsev *et al.*^{IV-3} to an analytical calculation of the central peak position in an infinite homogeneous thin superconducting strip. It was shown that in such a case the central peak was for any $J(B)$ dependence always located at zero applied magnetic field. Just granularity of the sample is the reason why the peak shifts to positive fields. In opposite, in a homogeneous sample with a finite aspect ratio the peak shifts to negative descending fields.¹¹

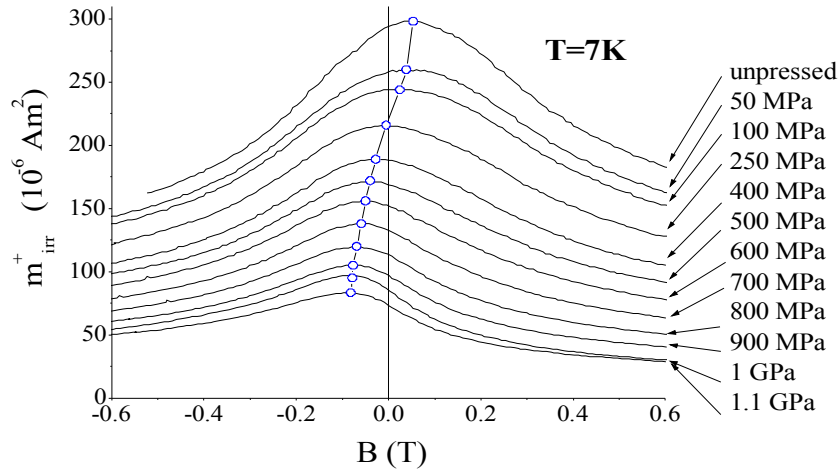


Fig. 15. The upper parts of MHLs measured on a Bi-2223/Ag tape measured after a load with different uniaxial stresses.

Although the tape bending proved that the intergranular currents were responsible for the anomaly, it was not clear to what extent the bending damaged intergrain links. Therefore, we performed a test of a tape by a uniaxial stress increasing by small steps.^{IV-4} In accordance with the increasing stress and the corresponding gradual damage of intergrain links, the magnetization loop gradually changed from anomalous to regular, central peak shifted to negative fields, and the average moment curve shifted from the 1st to 4th quadrant. The final stage was reached at 1 GPa (Fig.15), where the $M_{av}(B)$ curve (Fig. 16) started to go back to zero. Just the average moment line, calculated as a mean value of the upper and lower branch of the MHL, gave the best insight to the evolution of the anomaly. Note that this moment is close to the reversible moment obtained from field-cooled (FC) measurements, where the sample was first magnetized to the desired field value at a temperature above T_c and then cooled down up to some 5 K. The latter experiment, performed on an intact tape, showed that the FC reversible moment behaved irregularly only at the applied fields lower than $B_{irr}(T)$ at the given temperature. It indicates that magnetic flux is in the tapes **reversibly** redistributed

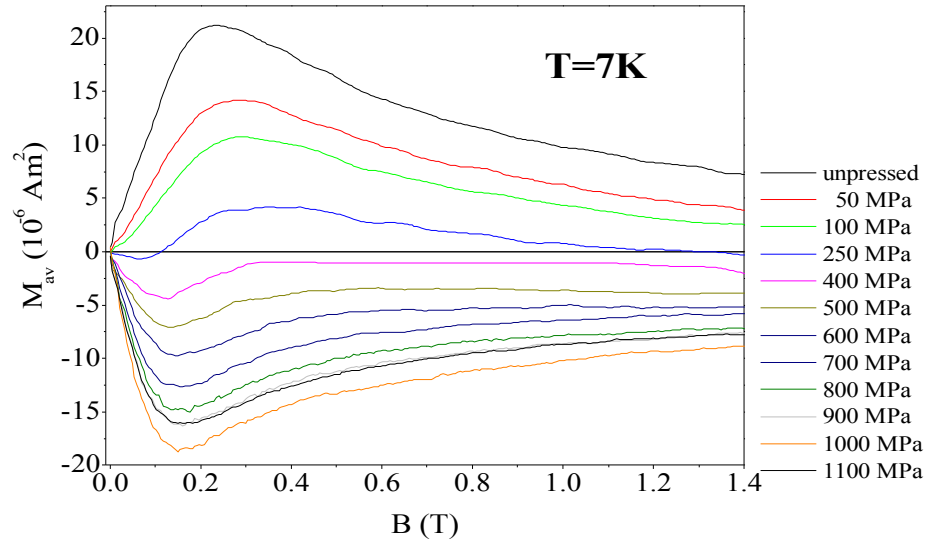


Fig. 16. An average magnetic moment as a function of applied field measured after the sample exposure to uniaxial stresses of indicated values. The moment develops from highly anomalous (positive in all fields) up to regular one, close to reversible moment of individual grains.

during field cooling and warming processes.

In order to better understand magnetic flux dynamics in granular materials, we studied the flux propagation on a relatively simple artificially granular thin film system. The first sample, prepared at the Chalmers University, Sweden, consisted of disks of about 50 μm in diameter (Fig. 17), close packed in hexagonal lattice, with contacts only 2-3 μm wide.^{IV-5} The idea was to visualize the flux dynamics by means of magneto-optical observation and compare it with the total magnetic moment measured by means of VSM. Similarly as in the Bi-based superconducting tapes, there were two systems of currents. The intragranular ones, screening the ‘grains’ from the gradually penetrating magnetic flux, and the intergranular currents flowing through the ‘intergrain’ contacts over the entire sample and screening the whole sample from the external magnetic field.

The latter ones were much lower than the intragranular ones but the final effect of both types of currents on the total magnetic moment was comparable due to their different loop perimeters (1 mm to 50 μm). Magnetization measurements showed a similar anomaly as described for the Bi-based tapes. It was another evidence that the anomaly is due to material granularity. Magneto-optical measurements revealed a much faster flux penetration through the intergranular space than into the grains interior. This behavior was attributed to much weaker screening by small intergranular currents. Our analysis of the flux penetration showed that the bridges had to be two-way paths for screening currents. The MO experiments indicated that the sample was not ideally homogeneous and magnetic flux penetrated its

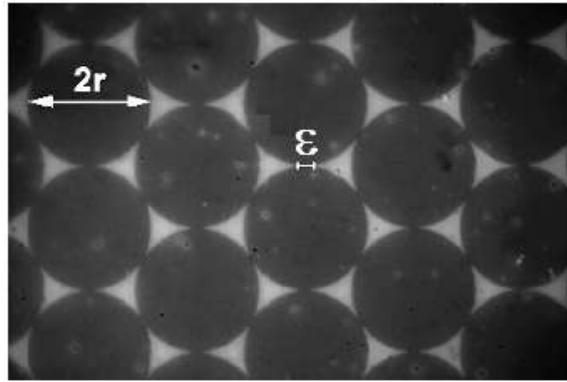


Fig. 17. SEM image of the model Y-123 hexagonal thin film structure consisting of disks 50 μm in diameter. The contact width is about 2-3 μm wide. The film thickness is 200 nm.

interior irregularly.^{IV-5}

This was caused by rather high demands on the thin film patterning precision with the given design. We therefore decided to prepare a new series of samples with a modified design. This plan was realized only recently, in collaboration with Research Center Julich (Dr. R. Wördenweber). In the Institute of Thin

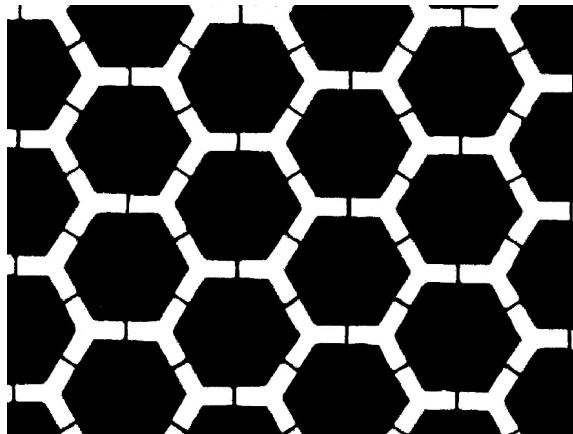


Fig. 18. Scheme of the hexagonal structure composed on a YBaCuO thin film 200 nm thick. The ‘grain’ dimension is 48 μm , the intergrain space 2 or 4 μm wide, the connecting bridges are 2 or 4 μm wide.

Films and Interfaces our doctoral student V. Yurchenko prepared a series of thin film samples consisting of close-packed structures of hexagonal grains of 48 μm size, 2 μm apart each other, interconnected by tiny bridges of different widths (Fig. 18).

Three samples with identical grains but different bridge widths, 4, 2, and 0 μm , were measured by VSM and magneto-optically.^{IV-6} The MO experiment was performed at University of Oslo. In the last case (reference sample without bridges) magnetic flux penetrated the intergranular space immediately after the field had been switched on. In the other two samples the flux front propagation velocity was inversely proportional to the bridge

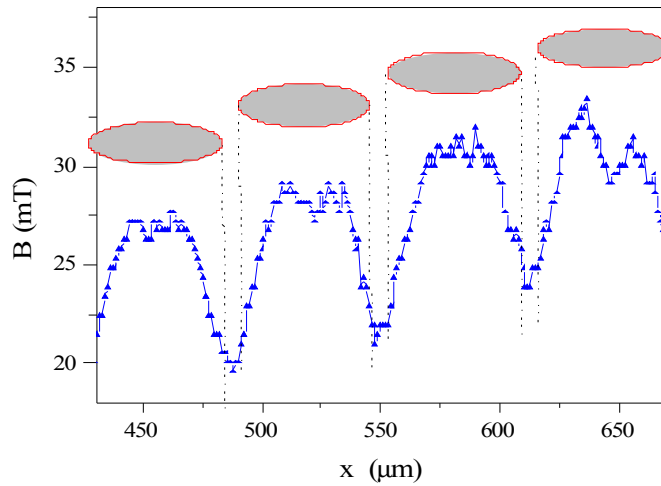


Fig. 19. Analysis of the magnetic flux profile after the field reversal from 45 mT to 15.6 mT. The ellipses indicate positions of the corresponding ‘grains’. The magnetic flux inside the grains is nearly constant.

width. Similarly as in the first model sample^{IV-5} the maximum magnetic field was not high enough to fully saturate the grains. However, after the field reversal the not yet penetrated grain centers were rapidly filled by the flux (Fig. 19). This phenomenon needs explanation. The much faster magnetic flux propagation into the intergranular space than into the grains implies that a certain part of the intergranular flux arises from an additional vortex nucleation in the inner parts of the sample (or in other words, from penetration along c-axis). A similar effect was simultaneously observed on thin film arrays of artificial defects, antidots.¹²

The total magnetic moments of the sample without bridges was rather small with respect to other two samples, where the intergranular current contribution was proportional to the

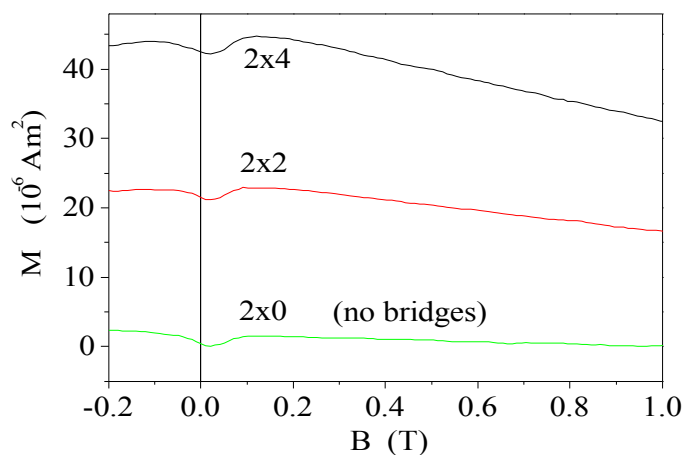


Fig. 20. The upper branches of the MHLs measured on three model samples consisting of the same grain systems with different widths of interconnecting bridges (as indicated in the figure (numbers in μm)). The anomalous position of the central peak was particularly evident after subtracting the lowest curve from the other two. The dip at zero field is evidently due to grains but its origin is not yet understood.

bridge width (Fig. 20). As expected, the central peak had an anomalous position in positive descending fields (evident in particular after the lowest curve subtraction from the upper two).

Summarizing the last part, one can say that thin film structures proved to be capable of modeling the much more complicated granular medium of Bi-based tapes. They can be easily investigated magneto-optically and magnetic flux dynamics can be studied on them in detail. The next step is to reach higher fields, in order to fully penetrate the superconducting ‘grains’. Another important task is to understand all the observed features. In this point the problem gets close to the tasks occurring in arrays of artificial defects, antidots, studied for electronic applications. This new field has attracted interest of my doctoral student Vitaliy Yurchenko, who just submitted his thesis on this subject for defense.

References

1. H.G. Schnack, R. Griessen, J.G. Lensink, Wen Hai-Hu, *Phys. Rev. B* 48, 13198 (1993)
2. A.D. Caplin, L.F. Cohen, G.K. Perkins, A.A. Zhukov, *Supercond. Sci. Technol.* 7, 412 (1994)
3. A. A. Zhukov, H. Küpfer, G. Perkins, L. F. Cohen, A. D. Caplin, S. A. Klestov, H. Claus, V. I. Voronkova, T. Wolf, and H. Wühl, *Phys. Rev. B* 51, 12704-12714 (1995).
4. A. Erb, J.-Y. Genoud, F. Marty, F. Däumling, E. Walker, R. Flückiger, *J. Low Temp. Phys.* 105, 1023 (1996).
5. H. Küpfer, Th. Wolf, C. Lessing, A. A. Zhukov, X. Lançon, R. Meier-Hirmer, W. Schauer, and H. Wühl, *Phys. Rev. B* 58, 2886-2894 (1998).
6. G. K. Perkins, L. F. Cohen, A. A. Zhukov, A. D. Caplin, *Phys. Rev. B* 51, 8513 (1995).
7. G. K. Perkins and A. D. Caplin, *Phys. Rev. B* 54, 12551 (1996)
8. F.M. Sauerzopf, H.P. Wiesinger, H.W. Weber, G.W. Crabtree, *Phys. Rev. B* 51, 6002 (1995).
9. F.M. Sauerzopf, *Phys. Rev. B* 57, 10959 (1998).
10. J. C. Phillips, *Physica C* 228, 171 (1994)
11. M. R. Koblischka, L. Pust, M. Jirsa, T. H. Johansen, *Physica C* 320 (1999) 101-104.
12. V. Yurchenko, P. Lahl, S. Bunte, M. Jirsa, R. Wördenweber, 3rd European Conference on Vortex Matter in Superconductors, Crete, Greece, September 20 – 28, 2003, *Physica C* 404, 426 (2004)

Publications constituting the thesis

I. Dynamic relaxation effect

- [I-1] L. Půst, J. Kadlecová, **M. Jirsa**, S. Durčok: Correlation between magnetic hysteresis and magnetic relaxation in YBaCuO single crystals. *J. Low Temp. Phys.* **78** (1990) 179-186.
[Impact factor 1.139, 57 citations]
- [I-2] L. Půst, **M. Jirsa**, J. Kadlecová, S. Durčok: Magnetic hysteresis loops and flux creep in single crystals of YBaCuO. Proc. 13th Int. Cryogenic Engin. Conf. (ICEC-13), Beijing (China), 24-27 April 1990, P18-4. *Cryogenics* **30** (1990) 886-890
[Impact factor 0.697, 7 citations]
- [I-3] L. Půst, **M. Jirsa**, R. Griessen, H.G. Schnack: Critical current relaxation in epitaxial thin YBaCuO films in changing and constant field. 4th World Congress on Superconductivity, Munich (Germany), September 14-18, 1992. *Appl. Superconductivity* **1** (1993) 835-844.
[Impact factor 0.763, 0 citations]
- [I-4] **M. Jirsa**, L. Půst, H.G. Schnack, R. Griessen: Extension of the time window for investigation of relaxation effects in high- T_c superconductors. *Physica C* **207** (1993) 85-96.
[Impact factor 0.806, 83 citations]
- [I-5] **M. Jirsa**, A. J. J. Van Dalen, M.R. Koblishka, G. Ravi Kumar, R. Griessen: Angle dependent superconducting current and relaxation in a twin-free DyBa₂Cu₃O_{7.8} single crystal. 7th Int. Workshop on Critical Currents (IWCC), Alpbach, Austria, 24-27 January 1994. In: Critical Currents in Superconductors, ed.: H.W. Weber, World Scientific 1994, 221-224.
3 citations
- [I-6] **M. Jirsa**, M.R. Koblishka, A. J. J. van Dalen: Relaxation and scaling of magnetization around the fishtail minimum in DyBaCuO single crystal with columnar tracks. *Supercond. Sci. Technol.* **10** (1997) 484-491.
[Impact factor 1.511, 1 citation]
-

II. $J(B)$ performance of untwinned bulk RE-123 superconductors

- [II-1] **M. Jirsa**, L. Půst, D. Dlouhý, M.R. Koblishka: Fishtail shape in the magnetic hysteresis loop for superconductors: Interplay between different pinning mechanisms. *Phys. Rev. B* **55** (1997) 3276-3284.
[Impact factor 3.070, 25 citations]
- [II-2] **M. Jirsa**, L. Půst: A comparative study of irreversible magnetization and pinning force density in (RE)Ba₂Cu₃O_{7.8} and some other high T_c compounds in view of a novel scaling scheme. *Physica C* **291** (1997) 17-24.
[Impact factor 0.806, 12 citations]
- [II-3] **M. Jirsa**, M. R. Koblishka, M. Muralidhar, T. Higuchi, and M. Murakami: Comparison of different approaches in modeling the fishtail shape in RE-123 bulk superconductors. *Physica C* **338** (2000) 235-245.
[Impact factor 0.806, 5 citations]

- [II-4] **M. Jirsa**, M. Muralidhar, M. Murakami, K. Noto, T. Nishizaki, and N. Kobayashi: J_c - B performance study of an OCMG (Nd-Eu-Gd)-123 material doped by sub-micron Gd-211 particles. *Supercond. Sci. Technol.* **14** (2001) 50-57
[Impact factor 1.511, 5 citations]
- [II-5] V. Zablotskii, **M. Jirsa**, P. Petrenko: Vortex pinning by large normal particles in high- T_c superconductors. *Phys. Rev. B* **65** (2002) 2245081-4
[Impact factor 3.070, 1 citation]
- [II-6] **M. Jirsa**, V. Zablotskii, T. Nishizaki, N. Kobayashi, M. Muralidhar, M. Murakami: Relaxation study of RE-123 materials with different types of pinning defects. *Physica C* **388-389** (2003) 683-684
[Impact factor 0.806, 0 citations]
- [II-7] **M. Jirsa**, T. Nishizaki, N. Kobayashi, M. Muralidhar, M. Murakami: Relaxation in bulk RE-123 superconductors. *Phys. Rev. B* (2004), in print
[Impact factor 3.070, 0 citations]
- [II-8] M. Muralidhar, N. Sakai, **M. Jirsa**, M. Murakami: Vortex pinning by mesoscopic defects - a way to levitation at liquid oxygen temperature. *Appl. Phys. Lett.* **83** (2003) 705-707
[Impact factor 3.849, 0 citations]
-

III. Twin structure effects in bulk RE-123 compounds

- [III-1] **M. Jirsa**, M. R. Koblishka, T. Higuchi, and M. Murakami: Effect of twin planes in the magnetization hysteresis loop of NdBa₂Cu₃O_y single crystal. *Phys. Rev. B* **58** (1998) R14771-4.
[Impact factor 3.070, 6 citations]
- [III-2] **M. Jirsa**, M. R. Koblishka, M. Murakami, G. Perkins, A. D. Caplin: Flux pinning by twin planes in Nd-123 and Y-123 single crystals. 22nd International Conference on Low Temperature Physics (LT22), Helsinki, Finland, August 4-11, 1999. *Physica B* **284-288** (2000) 851-852.
[Impact factor 0.806, 0 citations]
- [III-3] M. Muralidhar, N. Sakai, N. Chikumoto, **M. Jirsa**, T. Machi, M. Nishiyama, Y. Hu, and M. Murakami: New type of Vortex Pinning Structure Effective at Very High Magnetic Fields. *Phys. Rev. Letters* **89** (2002) 2370011-4
[Impact factor 6.668, 4 citations]
- [III-4] **M. Jirsa**, V. Zablotskii, M. Muralidhar, K. Iida, M. Murakami: Engineering of J_c - B characteristics of RE-Ba-Cu-O melt-textured superconductors. International Symposium on Superconductivity 2001, Kobe, Japan, September 25 - 27, 2001 *Physica C* **378-381** (2002) 707-712.
[Impact factor 0.806, 0 citations]
-

IV. Granular superconductors

- [IV-1] **M. Jirsa**, L. Půst, P. Nálezka, L. Papadimitriou, I. Samaras, O. Valassiades: Magnetic properties of YBa₂Cu₃Mg_xO_{7.8} ceramics. *Supercond. Sci. Technol.* **11** (1998) 757-765.

[Impact factor 1.511, 4 citations]

- [IV-2] P. Nalevka, **M. Jirsa**, L. Pust, A. Yu. Galkin, M. R. Koblishka, R. Flükiger: Detailed magnetisation study of inter- and intragranular currents in Ag-sheathed Bi-2223 tape. 3rd European Conference on Applied Superconductivity EUCAS'97, Veldhoven, 30 June- 3 July, 1997 In: Inst. Phys. Conf. Ser. No. 158 ed. IOP Publishing Ltd. 1997, pp. 1161-1164.

1 citation

- [IV-3] D.V. Shantsev, M.R. Koblishka, Y.M. Galperin, T.H. Johanson, L. Pust, and **M. Jirsa**: Central peak position in magnetisation loops of high- T_c superconductors. *Phys. Rev. Letters* **82** (1999) 2947-2950

[Impact factor 6.668, 14 citations]

- [IV-4] **M. Jirsa**, V. Yurchenko, V. Novák, P. Kováč, I. Hušek: Peculiarities of induced intergranular currents in Bi-2223/Ag tapes. 5th European Conference on Applied Superconductivity, August 26-30, 2001, Copenhagen, Denmark. *Physica C* **372-376** (2002) 1855-1858

[Impact factor 0.806, 0 citations]

- [IV-5] M. R. Koblishka, L. Pust, A. Galkin, P. Nalevka, **M. Jirsa**, T.H. Johansen, H. Bratsberg, B. Nilsson, and T. Claeson: Flux penetration into an artificial granular sample. *Phys. Rev. B* **59** (1999) 12114-12120

[Impact factor 3.070, 5 citations]

- [IV-6] **M. Jirsa**, V. Yurchenko, A. V. Bobyl, T. H. Johanson, D. Shantsev, R. Wordenweber: Magnetic flux dynamics in a hexagonal network of superconducting islands. 3rd European Conference on Vortex Matter in Superconductors, Crete (Greece), September 20-28, 2003 *Physica C* **404** (2004) 426-430

[Impact factor 0.806, 0 citations]